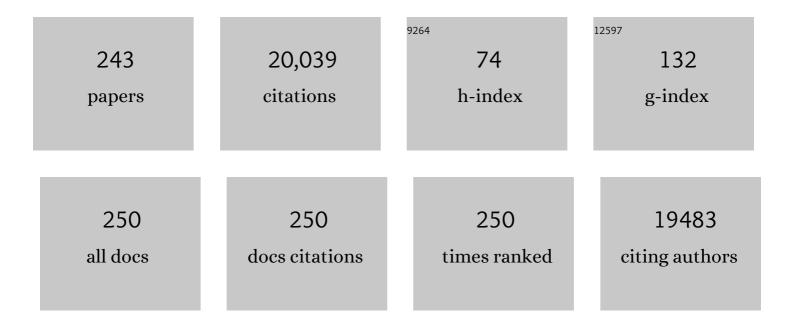
List of Publications by Year in descending order

Source: https://exaly.com/author-pdf/1861373/publications.pdf Version: 2024-02-01



WENLILL

#	Article	IF	CITATIONS
1	An integrated flexible film as cathode for High-Performance Lithium–Sulfur battery. Journal of Colloid and Interface Science, 2022, 606, 1627-1635.	9.4	7
2	Tunable active sites on biogas digestate derived biochar for sulfanilamide degradation by peroxymonosulfate activation. Journal of Hazardous Materials, 2022, 421, 126794.	12.4	75
3	Interwoven nickel(II)-dimethylglyoxime nanowires in 3D nickel foam for dendrite-free lithium deposition. Chinese Chemical Letters, 2022, 33, 2165-2170.	9.0	15
4	Organophosphorus Hybrid Solid Electrolyte Interphase Layer Based on Li <i>_x</i> PO ₄ Enables Uniform Lithium Deposition for Highâ€Performance Lithium Metal Batteries. Advanced Functional Materials, 2022, 32, 2107923.	14.9	27
5	Visible light photocatalytic degradation of sulfanilamide enhanced by Mo doping of BiOBr nanoflowers. Journal of Hazardous Materials, 2022, 424, 127563.	12.4	104
6	Synergistic interaction between inorganic layered materials and intumescent fire retardants for advanced fire protection. Carbon, 2022, 187, 290-301.	10.3	15
7	Ultrathin Aluminum Nanosheets Grown on Carbon Nanotubes for High Performance Lithium Ion Batteries. Advanced Functional Materials, 2022, 32, 2109112.	14.9	17
8	Toward stable zinc aqueous rechargeable batteries by anode morphology modulation via polyaspartic acid additive. Energy Storage Materials, 2022, 45, 777-785.	18.0	44
9	Organogel-assisted porous organic polymer embedding Cu NPs for selectivity control in the semi hydrogenation of alkynes. Nanoscale, 2022, 14, 1505-1519.	5.6	14
10	Synthetic solid oxide sorbents for CO ₂ capture: state-of-the art and future perspectives. Journal of Materials Chemistry A, 2022, 10, 1682-1705.	10.3	40
11	Accelerated Oxidation of Organic Micropollutants during Peracetic Acid Treatment in the Presence of Bromide Ions. ACS ES&T Water, 2022, 2, 320-328.	4.6	10
12	Application of Titanate Nanotubes for Photocatalytic Decontamination in Water: Challenges and Prospects. ACS ES&T Engineering, 2022, 2, 1015-1038.	7.6	24
13	Optimisation of syngas production from a novel two-step chemical looping reforming process using Fe-dolomite as oxygen carriers. Fuel Processing Technology, 2022, 228, 107169.	7.2	11
14	Hydrogen atom abstraction mechanism for organic compound oxidation by acetylperoxyl radical in Co(II)/peracetic acid activation system. Water Research, 2022, 212, 118113.	11.3	44
15	CO2 hydrogenation to methanol on tungsten-doped Cu/CeO2 catalysts. Applied Catalysis B: Environmental, 2022, 306, 121098.	20.2	50
16	Efficient ofloxacin degradation via photo-Fenton process over eco-friendly MIL-88A(Fe): Performance, degradation pathways, intermediate library establishment and toxicity evaluation. Environmental Research, 2022, 210, 112937.	7.5	25
17	Increasing oxygen vacancies in CeO ₂ nanocrystals by Ni doping and reduced graphene oxide decoration towards electrocatalytic hydrogen evolution. CrystEngComm, 2022, 24, 3369-3379.	2.6	9
18	Effect and Mechanism of Titanium Nanomaterials on Microbial Community Structure and Function in Sequencing Batch Reactor. ACS ES&T Water, 2022, 2, 395-404.	4.6	2

#	Article	IF	CITATIONS
19	Interface Engineering of Co(OH) ₂ Nanosheets Growing on the KNbO ₃ Perovskite Based on Electronic Structure Modulation for Enhanced Peroxymonosulfate Activation. Environmental Science & Technology, 2022, 56, 5200-5212.	10.0	136
20	Efficient activation of ferrate(VI) by colloid manganese dioxide: Comprehensive elucidation of the surface-promoted mechanism. Water Research, 2022, 215, 118243.	11.3	46
21	Life cycle climate change mitigation through next-generation urban waste recovery systems in high-density Asian cities: A Singapore Case Study. Resources, Conservation and Recycling, 2022, 181, 106265.	10.8	7
22	Concentrate and degrade PFOA with a photo-regenerable composite of In-doped TNTs@AC. Chemosphere, 2022, 300, 134495.	8.2	13
23	Blubber Cortisol-Based Approach to Explore the Endocrine Responses of Indo-Pacific Humpback Dolphins (<i>Sousa chinensis</i>) to Diet Shifts and Contaminant Exposure. Environmental Science & Technology, 2022, 56, 1069-1080.	10.0	11
24	Stabilizing single-atomic ruthenium by ferrous ion doped NiFe-LDH towards highly efficient and sustained water oxidation. Chemical Engineering Journal, 2022, 446, 136962.	12.7	25
25	Boosting Electrocatalytic Hydrogen Evolution with Anodic Oxidative Upgrading of Formaldehyde over Trimetallic Carbides. ACS Sustainable Chemistry and Engineering, 2022, 10, 7108-7116.	6.7	5
26	Effects of Molecular Structure on Organic Contaminants' Degradation Efficiency and Dominant ROS in the Advanced Oxidation Process with Multiple ROS. Environmental Science & Technology, 2022, 56, 8784-8795.	10.0	161
27	Breaking the Stoichiometric Limit in Oxygen-Carrying Capacity of Fe-Based Oxygen Carriers for Chemical Looping Combustion using the Mg-Fe-O Solid Solution System. ACS Sustainable Chemistry and Engineering, 2022, 10, 7242-7252.	6.7	6
28	<i>In-Situ</i> Construction of Ceramic–Polymer All-Solid-State Electrolytes for High-Performance Room-Temperature Lithium Metal Batteries. , 2022, 4, 1297-1305.		13
29	Regulation of Zinc Interface by Maltitol for Long-Life Dendrite-free Aqueous Zinc Ion Batteries. Journal of Electronic Materials, 2022, 51, 4763-4771.	2.2	5
30	Designing Anion-Derived Solid Electrolyte Interphase in a Siloxane-Based Electrolyte for Lithium-Metal Batteries. ACS Applied Materials & Interfaces, 2022, 14, 27873-27881.	8.0	23
31	Constructing a lithiophilic and mixed conductive interphase layer in electrolyte with dual-anion solvation sheath for stable lithium metal anode. Energy Storage Materials, 2022, 50, 792-801.	18.0	14
32	Unraveling the Unique Role of Methyl Position on the Ring-Opening Barrier in Photocatalytic Decomposition of Xylene Isomers. ACS Catalysis, 2022, 12, 8363-8371.	11.2	8
33	Asymmetric double-layer composite electrolyte with enhanced ionic conductivity and interface stability for all-solid-state lithium metal batteries. Chinese Chemical Letters, 2021, 32, 125-131.	9.0	45
34	Bifunctional Bi12O17Cl2/MIL-100(Fe) composites toward photocatalytic Cr(VI) sequestration and activation of persulfate for bisphenol A degradation. Science of the Total Environment, 2021, 752, 141901.	8.0	175
35	Advanced electrolyte design for stable lithium metal anode: From liquid to solid. Nano Energy, 2021, 80, 105516.	16.0	111
36	Insights into catalytic activation of peroxymonosulfate for carbamazepine degradation by MnO2 nanoparticles in-situ anchored titanate nanotubes: Mechanism, ecotoxicity and DFT study. Journal of Hazardous Materials, 2021, 402, 123779.	12.4	141

#	Article	IF	CITATIONS
37	Engineering the interface between LiCoO ₂ and Li ₁₀ GeP ₂ S ₁₂ solid electrolytes with an ultrathin Li ₂ CoTi ₃ O ₈ interlayer to boost the performance of all-solid-state batteries. Energy and Environmental Science, 2021, 14, 437-450.	30.8	82
38	Bulk and surface degradation in layered Ni-rich cathode for Li ions batteries: Defect proliferation via chain reaction mechanism. Energy Storage Materials, 2021, 35, 62-69.	18.0	46
39	Photo-ammonification of low molecular weight dissolved organic nitrogen by direct and indirect photolysis. Science of the Total Environment, 2021, 764, 142930.	8.0	8
40	Facile synthesis of sulfhydryl modified covalent organic frameworks for high efficient Hg(II) removal from water. Journal of Hazardous Materials, 2021, 405, 124190.	12.4	46
41	PtPdCu cubic nanoframes as electrocatalysts for methanol oxidation reaction. CrystEngComm, 2021, 23, 7978-7984.	2.6	5
42	Experimental and computational assessment of 1,4-Dioxane degradation in a photo-Fenton reactive ceramic membrane filtration process. Frontiers of Environmental Science and Engineering, 2021, 15, 1.	6.0	14
43	Layered double hydroxide-based electrocatalysts for the oxygen evolution reaction: identification and tailoring of active sites, and superaerophobic nanoarray electrode assembly. Chemical Society Reviews, 2021, 50, 8790-8817.	38.1	331
44	An aqueous polyethylene oxide-based solid-state electrolyte with high voltage stability for dendrite-free lithium deposition <i>via</i> a self-healing electrostatic shield. Dalton Transactions, 2021, 50, 14296-14302.	3.3	7
45	Controlling lattice oxygen activity of oxygen carrier materials by design: a review and perspective. Reaction Chemistry and Engineering, 2021, 6, 1527-1537.	3.7	21
46	CO2 Capture for Dry Reforming of Natural Gas: Performance and Process Modeling of Calcium Carbonate Looping Using Acid Based CaCO3 Sorbent. Frontiers in Energy Research, 2021, 8, .	2.3	2
47	Silicate-Enhanced Heterogeneous Flow-Through Electro-Fenton System Using Iron Oxides under Nanoconfinement. Environmental Science & Technology, 2021, 55, 4045-4053.	10.0	192
48	A new multi-party quantum private comparison based on n-dimensional n-particle GHZ state. Modern Physics Letters A, 2021, 36, 2150083.	1.2	3
49	Recent Progress of the Design and Engineering of Bismuth Oxyhalides for Photocatalytic Nitrogen Fixation. Advanced Energy and Sustainability Research, 2021, 2, 2000097.	5.8	14
50	Superwetting behaviors at the interface between electrode and electrolyte. Cell Reports Physical Science, 2021, 2, 100374.	5.6	22
51	Enhanced Oxidation of Organic Contaminants by Iron(II)-Activated Periodate: The Significance of High-Valent Iron–Oxo Species. Environmental Science & Technology, 2021, 55, 7634-7642.	10.0	208
52	Tunable Covalent Organic Frameworks with Different Heterocyclic Nitrogen Locations for Efficient Cr(VI) Reduction, <i>Escherichia coli</i> Disinfection, and Paracetamol Degradation under Visible-Light Irradiation. Environmental Science & Technology, 2021, 55, 5371-5381.	10.0	79
53	Simple Mix-and-Read Assay with Multiple Cyclic Enzymatic Repairing Amplification for Rapid and Sensitive Detection of DNA Glycosylase. Analytical Chemistry, 2021, 93, 6913-6918.	6.5	24
54	Uptake, excretion and toxicity of titanate nanotubes in three stains of free-living ciliates of the genus Tetrahymena. Aquatic Toxicology, 2021, 233, 105790.	4.0	7

#	Article	IF	CITATIONS
55	A novel electrocatalytic filtration system with carbon nanotube supported nanoscale zerovalent copper toward ultrafast oxidation of organic pollutants. Water Research, 2021, 194, 116961.	11.3	123
56	Insights into the Electron-Transfer Mechanism of Permanganate Activation by Graphite for Enhanced Oxidation of Sulfamethoxazole. Environmental Science & Technology, 2021, 55, 9189-9198.	10.0	131
57	Ultrafast fluorescent probe with near-infrared analytical wavelength for fluoride ion detection in real samples. Spectrochimica Acta - Part A: Molecular and Biomolecular Spectroscopy, 2021, 252, 119518.	3.9	12
58	Aerophilic Co-Embedded N-Doped Carbon Nanotube Arrays as Highly Efficient Cathodes for Aluminum–Air Batteries. ACS Applied Materials & Interfaces, 2021, 13, 26853-26860.	8.0	15
59	Hollow Carbon Spheres Embedded with VN Quantum Dots as an Efficient Cathode Host for Lithium–Sulfur Batteries. Energy & Fuels, 2021, 35, 10219-10226.	5.1	17
60	Surface modification of BiOBr/TiO2 by reduced AgBr for solar-driven PAHs degradation: Mechanism insight and application assessment. Journal of Hazardous Materials, 2021, 412, 125221.	12.4	58
61	Strong Metal–Support Interaction for 2D Materials: Application in Noble Metal/TiB ₂ Heterointerfaces and their Enhanced Catalytic Performance for Formic Acid Dehydrogenation. Advanced Materials, 2021, 33, e2101536.	21.0	47
62	The degradation pathways of carbamazepine in advanced oxidation process: A mini review coupled with DFT calculation. Science of the Total Environment, 2021, 779, 146498.	8.0	88
63	Iron-Catalyzed Enantioselective Radical Carboazidation and Diazidation of $\hat{I}\pm,\hat{I}^2$ -Unsaturated Carbonyl Compounds. Journal of the American Chemical Society, 2021, 143, 11856-11863.	13.7	50
64	Different degradation mechanisms of carbamazepine and diclofenac by single-atom Barium embedded g-C3N4: the role of photosensitation-like mechanism. Journal of Hazardous Materials, 2021, 416, 125936.	12.4	43
65	Highly efficient AgBr/h-MoO3 with charge separation tuning for photocatalytic degradation of trimethoprim: Mechanism insight and toxicity assessment. Science of the Total Environment, 2021, 781, 146754.	8.0	38
66	Redox chemistry of N4-Fe2+ in iron phthalocyanines for oxygen reduction reaction. Chinese Journal of Catalysis, 2021, 42, 1404-1412.	14.0	33
67	Insights into the role of in-situ and ex-situ hydrogen peroxide for enhanced ferrate(VI) towards oxidation of organic contaminants. Water Research, 2021, 203, 117548.	11.3	72
68	Insight into the synergetic effect of photocatalysis and transition metal on sulfite activation: Different mechanisms for carbamazepine and diclofenac degradation. Science of the Total Environment, 2021, 787, 147626.	8.0	21
69	High-performance aqueous polysulfide-iodide flow battery realized by an efficient bifunctional catalyst based on copper sulfide. Materials Today Energy, 2021, 21, 100746.	4.7	14
70	Coupling chemical looping combustion of solid fuels with advanced steam cycles for CO2 capture: A process modelling study. Energy Conversion and Management, 2021, 244, 114455.	9.2	30
71	Oxygen defective titanate nanotubes induced by iron deposition for enhanced peroxymonosulfate activation and acetaminophen degradation: Mechanisms, water chemistry effects, and theoretical calculation. Journal of Hazardous Materials, 2021, 418, 126180.	12.4	33
72	From dendritic mesoporous silica microspheres to waxberry-like hierarchical hollow carbon spheres: rational design of carbon host for lithium sulfur batteries. Nanotechnology, 2021, 32, 485405.	2.6	0

#	Article	IF	CITATIONS
73	Ni/Hydrochar Nanostructures Derived from Biomass as Catalysts for H2 Production through Aqueous-Phase Reforming of Methanol. ACS Applied Nano Materials, 2021, 4, 8958-8971.	5.0	6
74	Recycling-oriented cathode materials design for lithium-ion batteries: Elegant structures versus complicated compositions. Energy Storage Materials, 2021, 41, 380-394.	18.0	46
75	Intensified solar thermochemical CO2 splitting over iron-based redox materials via perovskite-mediated dealloying-exsolution cycles. Chinese Journal of Catalysis, 2021, 42, 2049-2058.	14.0	13
76	Single-step production of hydrogen-rich syngas from toluene using multifunctional Ni-dolomite catalysts. Chemical Engineering Journal, 2021, 425, 131522.	12.7	17
77	A mixed ion-electron conducting network derived from a porous CoP film for stable lithium metal anodes. Materials Chemistry Frontiers, 2021, 5, 5486-5496.	5.9	7
78	Catalytic separators with Co–N–C nanoreactors for high-performance lithium–sulfur batteries. Inorganic Chemistry Frontiers, 2021, 8, 3066-3076.	6.0	29
79	Elucidating the Strain–Vacancy–Activity Relationship on Structurally Deformed Co@CoO Nanosheets for Aqueous Phase Reforming of Formaldehyde. Small, 2021, 17, e2102970.	10.0	29
80	MoSx microgrid electrodes with geometric jumping effect for enhancing hydrogen evolution efficiency. Science China Materials, 2021, 64, 892-898.	6.3	3
81	Catalytic Asymmetric Halogenation/Semipinacol Rearrangement of 3â€Hydroxylâ€3â€vinyl Oxindoles: A Stereodivergent Kinetic Resolution Process. Angewandte Chemie - International Edition, 2021, 60, 26599-26603.	13.8	18
82	Catalytic Asymmetric Halogenation/Semipinacol Rearrangement of 3â€Hydroxylâ€3â€vinyl Oxindoles: A Stereodivergent Kinetic Resolution Process. Angewandte Chemie, 2021, 133, 26803.	2.0	3
83	Correlation of Active Sites to Generated Reactive Species and Degradation Routes of Organics in Peroxymonosulfate Activation by Co-Loaded Carbon. Environmental Science & Technology, 2021, 55, 16163-16174.	10.0	189
84	Sorption of dispersed petroleum hydrocarbons by activated charcoals: Effects of oil dispersants. Environmental Pollution, 2020, 256, 113416.	7.5	23
85	The chemistry, recent advancements and activity descriptors for macrocycles based electrocatalysts in oxygen reduction reaction. Coordination Chemistry Reviews, 2020, 402, 213047.	18.8	78
86	Porous tube-like ZnS derived from rod-like ZIF-L for photocatalytic Cr(VI) reduction and organic pollutants degradation. Environmental Pollution, 2020, 256, 113417.	7.5	55
87	Carbon quantum dots modified tubular g-C3N4 with enhanced photocatalytic activity for carbamazepine elimination: Mechanisms, degradation pathway and DFT calculation. Journal of Hazardous Materials, 2020, 381, 120957.	12.4	134
88	ZnCo2O4/ZnO induced lithium deposition in multi-scaled carbon/nickel frameworks for dendrite-free lithium metal anode. Journal of Energy Chemistry, 2020, 43, 16-23.	12.9	39
89	Co-pyrolysis of sewage sludge and hydrochar with coals: Pyrolytic behaviors and kinetics analysis using TG-FTIR and a discrete distributed activation energy model. Energy Conversion and Management, 2020, 203, 112226.	9.2	43
90	Decipher of the structure and surface chemistry in molybdenum phosphosulfide on electrochemical catalytic hydrogen evolution reaction. Journal of Catalysis, 2020, 382, 228-236.	6.2	12

#	Article	IF	CITATIONS
91	Magnetic Fe3O4-deposited flower-like MoS2 nanocomposites for the Fenton-like Escherichia coli disinfection and diclofenac degradation. Journal of Hazardous Materials, 2020, 385, 121604.	12.4	116
92	Synthesis and Properties of Stable Sub-2-nm-Thick Aluminum Nanosheets: Oxygen Passivation and Two-Photon Luminescence. CheM, 2020, 6, 448-459.	11.7	15
93	Modification of zero valent iron nanoparticles by sodium alginate and bentonite: Enhanced transport, effective hexavalent chromium removal and reduced bacterial toxicity. Journal of Hazardous Materials, 2020, 388, 121822.	12.4	52
94	Ultrasonic stimulation of the brain to enhance the release of dopamine – A potential novel treatment for Parkinson's disease. Ultrasonics Sonochemistry, 2020, 63, 104955.	8.2	25
95	Deep-blue fluorescent emitter based on a 9,9-dioctylfluorene bridge with a hybridized local and charge-transfer excited state for organic light-emitting devices with EQE exceeding 8%. Journal of Materials Chemistry C, 2020, 8, 14117-14124.	5.5	34
96	Barium aluminate improved iron ore for the chemical looping combustion of syngas. Applied Energy, 2020, 272, 115236.	10.1	29
97	Developing Oxygen Carriers for Chemical Looping Biomass Processing: Challenges and Opportunities. Advanced Sustainable Systems, 2020, 4, 2000099.	5.3	26
98	Thiolâ€Branched Solid Polymer Electrolyte Featuring High Strength, Toughness, and Lithium Ionic Conductivity for Lithiumâ€Metal Batteries. Advanced Materials, 2020, 32, e2001259.	21.0	139
99	Oxygen-mediated water splitting on metal-free heterogeneous photocatalyst under visible light. Applied Catalysis B: Environmental, 2020, 279, 119378.	20.2	14
100	A concentrate-and-destroy technique for degradation of perfluorooctanoic acid in water using a new adsorptive photocatalyst. Water Research, 2020, 185, 116219.	11.3	87
101	Photocatalytic transformation fate and toxicity of ciprofloxacin related to dissociation species: Experimental and theoretical evidences. Water Research, 2020, 185, 116286.	11.3	99
102	Removal of 17β-Estradiol by Activated Charcoal Supported Titanate Nanotubes (TNTs@AC) through Initial Adsorption and Subsequent Photo-Degradation: Intermediates, DFT calculation, and Mechanisms. Water (Switzerland), 2020, 12, 2121.	2.7	9
103	Construction of a sensitive protease sensor with DNA-peptide conjugates for single-molecule detection of multiple matrix metalloproteinases. Biosensors and Bioelectronics, 2020, 169, 112647.	10.1	18
104	Synthesizing Highâ€Volume Chemicals from CO ₂ without Direct H ₂ Input. ChemSusChem, 2020, 13, 6066-6089.	6.8	15
105	Asymmetric Catalytic Synthesis of Epoxides via Three-Component Reaction of Diazoacetates, 2-Oxo-3-ynoates, and Nitrosoarenes. Organic Letters, 2020, 22, 6744-6749.	4.6	10
106	Agl modified covalent organic frameworks for effective bacterial disinfection and organic pollutant degradation under visible light irradiation. Journal of Hazardous Materials, 2020, 398, 122865.	12.4	73
107	High performance Ni catalysts prepared by freeze drying for efficient dry reforming of methane. Applied Catalysis B: Environmental, 2020, 275, 119109.	20.2	60
108	An asymmetric quasi-solid electrolyte for high-performance Li metal batteries. Chemical Communications, 2020, 56, 7195-7198.	4.1	14

#	Article	IF	CITATIONS
109	Atomically Dispersed Fe-N4 Modified with Precisely Located S for Highly Efficient Oxygen Reduction. Nano-Micro Letters, 2020, 12, 116.	27.0	99
110	Visible-Light-Driven Nitrogen Fixation Catalyzed by Bi ₅ O ₇ Br Nanostructures: Enhanced Performance by Oxygen Vacancies. Journal of the American Chemical Society, 2020, 142, 12430-12439.	13.7	260
111	Hydrogen bonding rather than cation bridging promotes graphene oxide attachment to lipid membranes in the presence of heavy metals. Environmental Science: Nano, 2020, 7, 2240-2251.	4.3	5
112	Pre-accumulation and in-situ destruction of diclofenac by a photo-regenerable activated carbon fiber supported titanate nanotubes composite material: Intermediates, DFT calculation, and ecotoxicity. Journal of Hazardous Materials, 2020, 400, 123225.	12.4	86
113	Cobalt/Peracetic Acid: Advanced Oxidation of Aromatic Organic Compounds by Acetylperoxyl Radicals. Environmental Science & Technology, 2020, 54, 5268-5278.	10.0	200
114	Single-atom silver induced amorphization of hollow tubular g-C3N4 for enhanced visible light-driven photocatalytic degradation of naproxen. Science of the Total Environment, 2020, 742, 140642.	8.0	34
115	Surface engineering of LiNi0.8Mn0.1Co0.1O2 towards boosting lithium storage: Bimetallic oxides versus monometallic oxides. Nano Energy, 2020, 77, 105034.	16.0	78
116	Piezo-activation of peroxymonosulfate for benzothiazole removal in water. Journal of Hazardous Materials, 2020, 393, 122448.	12.4	102
117	Metagenomic insights into the profile of antibiotic resistomes in a large drinking water reservoir. Environment International, 2020, 136, 105449.	10.0	65
118	Hollow-Structured Layered Double Hydroxide: Structure Evolution Induced by Gradient Composition. Inorganic Chemistry, 2020, 59, 1804-1809.	4.0	10
119	Radical attack and mineralization mechanisms on electrochemical oxidation of p-substituted phenols at boron-doped diamond anodes. Chemosphere, 2020, 248, 126033.	8.2	22
120	Porousâ€Organicâ€Polymerâ€Triggered Advancement of Sustainable Magnetic Efficient Catalyst for Chemoselective Hydrogenation of Cinnamaldehyde. ChemCatChem, 2020, 12, 3687-3704.	3.7	24
121	Superior removal of inorganic and organic arsenic pollutants from water with MIL-88A(Fe) decorated on cotton fibers. Chemosphere, 2020, 254, 126829.	8.2	93
122	Synchronous degradation of aqueous benzotriazole and bromate reduction in catalytic ozonation: Effect of matrix factor, degradation mechanism and application strategy in water treatment. Science of the Total Environment, 2020, 727, 138696.	8.0	13
123	Sale-based estimation of pharmaceutical concentrations and associated environmental risk in the Japanese wastewater system. Environment International, 2020, 139, 105690.	10.0	35
124	Novel CuCo ₂ O ₄ Composite Spinel with a Meso-Macroporous Nanosheet Structure for Sulfate Radical Formation and Benzophenone-4 Degradation: Interface Reaction, Degradation Pathway, and DFT Calculation. ACS Applied Materials & Interfaces, 2020, 12, 20522-20535.	8.0	83
125	Recent Advances in Nonâ€Precious Metalâ€Based Electrodes for Alkaline Water Electrolysis. ChemNanoMat, 2020, 6, 336-355.	2.8	92
126	Lithiophilic 3D SnS ₂ @Carbon Fiber Cloth for Stable Li Metal Anode. Wuli Huaxue Xuebao/ Acta Physico - Chimica Sinica, 2020, .	4.9	5

#	Article	IF	CITATIONS
127	Porous Copper Foam Co-operation with Thiourea for Dendrite-free Lithium Metal Anode. Wuli Huaxue Xuebao/ Acta Physico - Chimica Sinica, 2020, .	4.9	2
128	Zn Doped NiMn-Layered Double Hydroxide for High Performance Ni–Zn Battery. Journal of the Electrochemical Society, 2020, 167, 160550.	2.9	4
129	Promoting electrochemical conversion of CO2 to formate with rich oxygen vacancies in nanoporous tin oxides. Chinese Chemical Letters, 2019, 30, 2274-2278.	9.0	35
130	Hierarchical cobalt oxide@Nickel-vanadium layer double hydroxide core/shell nanowire arrays with enhanced areal specific capacity for nickel–zinc batteries. Journal of Power Sources, 2019, 436, 226867.	7.8	48
131	Aging amorphous/crystalline heterophase PdCu nanosheets for catalytic reactions. National Science Review, 2019, 6, 955-961.	9.5	75
132	Highly active WO3@anatase-SiO2 aerogel for solar-light-driven phenanthrene degradation: Mechanism insight and toxicity assessment. Water Research, 2019, 162, 369-382.	11.3	225
133	Surface-Based Li ⁺ Complex Enables Uniform Lithium Deposition for Stable Lithium Metal Anodes. ACS Applied Energy Materials, 2019, 2, 4602-4608.	5.1	32
134	Dendriteâ€Free Lithium Deposition via a Superfilling Mechanism for Highâ€Performance Liâ€Metal Batteries. Advanced Materials, 2019, 31, e1903248.	21.0	106
135	Role of sludge retention time in mitigation of nitrous oxide emission from a pilot-scale oxidation ditch. Bioresource Technology, 2019, 292, 121961.	9.6	22
136	Synergistic effect of hydrothermal co-carbonization of sewage sludge with fruit and agricultural wastes on hydrochar fuel quality and combustion behavior. Waste Management, 2019, 100, 171-181.	7.4	107
137	Research Progress of the Solid State Lithium-Sulfur Batteries. Frontiers in Energy Research, 2019, 7, .	2.3	39
138	Superaerophilic copper nanowires for efficient and switchable CO ₂ electroreduction. Nanoscale Horizons, 2019, 4, 490-494.	8.0	39
139	The effects of graphene oxide on nitrification and N2O emission: Dose and exposure time dependent. Environmental Pollution, 2019, 252, 960-966.	7.5	18
140	Asymmetric Synthesis of α,β-Epoxy-γ-lactams through Tandem Darzens/Hemiaminalization Reaction. Organic Letters, 2019, 21, 4713-4716.	4.6	17
141	Preparation and electro responsive properties of Mg-doped BaTiO3 with novel morphologies. Journal of Materials Science: Materials in Electronics, 2019, 30, 12107-12112.	2.2	5
142	Graphene modified anatase/titanate nanosheets with enhanced photocatalytic activity for efficient degradation of sulfamethazine under simulated solar light. Chemosphere, 2019, 233, 198-206.	8.2	60
143	Engineering Interfacial Aerophilicity of Nickel-Embedded Nitrogen-Doped CNTs for Electrochemical CO ₂ Reduction. ACS Applied Energy Materials, 2019, 2, 3991-3998.	5.1	23
144	A nickel(<scp>ii</scp>)-catalyzed asymmetric intramolecular Alder-ene reaction of 1,7-dienes. Chemical Communications, 2019, 55, 4479-4482.	4.1	16

#	Article	IF	CITATIONS
145	Vertical profile of soil/sediment pollution and microbial community change by e-waste recycling operation. Science of the Total Environment, 2019, 669, 1001-1010.	8.0	37
146	A general route <i>via</i> formamide condensation to prepare atomically dispersed metal–nitrogen–carbon electrocatalysts for energy technologies. Energy and Environmental Science, 2019, 12, 1317-1325.	30.8	290
147	Simultaneous Cr(VI) reduction and Cr(III) removal of bifunctional MOF/Titanate nanotube composites. Environmental Pollution, 2019, 249, 502-511.	7.5	97
148	Unveiling the Interfacial Effects for Enhanced Hydrogen Evolution Reaction on MoS ₂ /WTe ₂ Hybrid Structures. Small, 2019, 15, e1900078.	10.0	58
149	Boosting oxygen evolution of single-atomic ruthenium through electronic coupling with cobalt-iron layered double hydroxides. Nature Communications, 2019, 10, 1711.	12.8	446
150	An Entangled Cobalt–Nitrogen–Carbon Nanotube Array Electrode with Synergetic Confinement and Electrocatalysis of Polysulfides for Stable Li–S Batteries. ACS Applied Energy Materials, 2019, 2, 2904-2912.	5.1	28
151	Surface Restraint Synthesis of an Organic–Inorganic Hybrid Layer for Dendrite-Free Lithium Metal Anode. ACS Applied Materials & Interfaces, 2019, 11, 8717-8724.	8.0	39
152	Efficient removal of dyes from dyeing wastewater by powder activated charcoal/titanate nanotube nanocomposites: adsorption and photoregeneration. Environmental Science and Pollution Research, 2019, 26, 10263-10273.	5.3	28
153	Endoscopic dacryocystorhinostomy to treat congenital nasolacrimal canal dysplasia: a retrospective analysis in 40 children. BMC Ophthalmology, 2019, 19, 244.	1.4	4
154	Influences of isolated fractions of natural organic matter on adsorption of Cu(II) by titanate nanotubes. Science of the Total Environment, 2019, 650, 1412-1418.	8.0	27
155	Visible-light-driven photocatalytic degradation of diclofenac by carbon quantum dots modified porous g-C3N4: Mechanisms, degradation pathway and DFT calculation. Water Research, 2019, 151, 8-19.	11.3	520
156	Selectivity regulation of CO2 electroreduction through contact interface engineering on superwetting Cu nanoarray electrodes. Nano Research, 2019, 12, 345-349.	10.4	80
157	Phase interactions in Ni-Cu-Al2O3 mixed oxide oxygen carriers for chemical looping applications. Applied Energy, 2019, 236, 635-647.	10.1	33
158	Janus electrode with simultaneous management on gas and liquid transport for boosting oxygen reduction reaction. Nano Research, 2019, 12, 177-182.	10.4	43
159	Nitrogen-doped tungsten carbide nanoarray as an efficient bifunctional electrocatalyst for water splitting in acid. Nature Communications, 2018, 9, 924.	12.8	571
160	Dominant role of ammonia-oxidizing bacteria in nitrification due to ammonia accumulation in sediments of Danjiangkou reservoir, China. Applied Microbiology and Biotechnology, 2018, 102, 3399-3410.	3.6	30
161	Revealing the Contribution of Individual Factors to Hydrogen Evolution Reaction Catalytic Activity. Advanced Materials, 2018, 30, e1706076.	21.0	86
162	High-Performance Ni–Fe Redox Catalysts for Selective CH ₄ to Syngas Conversion via Chemical Looping. ACS Catalysis, 2018, 8, 1748-1756.	11.2	72

#	Article	IF	CITATIONS
163	Tuning Electronic Structure of NiFe Layered Double Hydroxides with Vanadium Doping toward High Efficient Electrocatalytic Water Oxidation. Advanced Energy Materials, 2018, 8, 1703341.	19.5	505
164	Biosynthesis of palladium nanoparticles using <i>Shewanella loihica</i> PV-4 for excellent catalytic reduction of chromium(<scp>vi</scp>). Environmental Science: Nano, 2018, 5, 730-739.	4.3	64
165	Surface Chemistry in Cobalt Phosphide-Stabilized Lithium–Sulfur Batteries. Journal of the American Chemical Society, 2018, 140, 1455-1459.	13.7	393
166	Analysis of CDK2 mutations in Chinese men with non-obstructive azoospermia who underwent testis biopsy. Reproductive BioMedicine Online, 2018, 36, 356-360.	2.4	5
167	Sea-Buckthorn-Like MnO ₂ Decorated Titanate Nanotubes with Oxidation Property and Photocatalytic Activity for Enhanced Degradation of 17β-Estradiol under Solar Light. ACS Applied Energy Materials, 2018, 1, 2123-2133.	5.1	34
168	Stable Li metal anode with protected interface for high-performance Li metal batteries. Energy Storage Materials, 2018, 15, 249-256.	18.0	89
169	Facile synthesis of magnetic Fe3O4@BiOI@AgI for water decontamination with visible light irradiation: Different mechanisms for different organic pollutants degradation and bacterial disinfection. Water Research, 2018, 137, 120-129.	11.3	117
170	Photocatalysis of bisphenol A by an easy-settling titania/titanate composite: Effects of water chemistry factors, degradation pathway and theoretical calculation. Environmental Pollution, 2018, 232, 580-590.	7.5	116
171	Singleâ€Crystalline Ultrathin Co ₃ O ₄ Nanosheets with Massive Vacancy Defects for Enhanced Electrocatalysis. Advanced Energy Materials, 2018, 8, 1701694.	19.5	451
172	Stable interstitial layer to alleviate fatigue fracture of high nickel cathode for lithium-ion batteries. Journal of Power Sources, 2018, 376, 200-206.	7.8	32
173	Co/CoP embedded in a hairy nitrogen-doped carbon polyhedron as an advanced tri-functional electrocatalyst. Materials Horizons, 2018, 5, 108-115.	12.2	184
174	Polyvinylchloride-derived N, S co-doped carbon as an efficient sulfur host for high-performance Li–S batteries. RSC Advances, 2018, 8, 37811-37816.	3.6	10
175	Newly designed primer pair revealed dominant and diverse comammox amoA gene in full-scale wastewater treatment plants. Bioresource Technology, 2018, 270, 580-587.	9.6	107
176	SnO2 quantum dots @ 3D sulfur-doped reduced graphene oxides as active and durable anode for lithium ion batteries. Electrochimica Acta, 2018, 291, 24-30.	5.2	37
177	Effect of carbon coating on the crystal orientation and electrochemical performance of nanocrystalline LiFePO4. Solid State Ionics, 2018, 327, 11-17.	2.7	20
178	Copper-Catalyzed Asymmetric Addition of Tertiary Carbon Nucleophiles to 2 <i>H</i> -Azirines: Access to Chiral Aziridines with Vicinal Tetrasubstituted Stereocenters. Organic Letters, 2018, 20, 5601-5605.	4.6	32
179	Structure and Electrocatalytic Reactivity of Cobalt Phosphosulfide Nanomaterials. Topics in Catalysis, 2018, 61, 958-964.	2.8	18
180	Activating basal plane in NiFe layered double hydroxide by Mn ²⁺ doping for efficient and durable oxygen evolution reaction. Nanoscale Horizons, 2018, 3, 532-537.	8.0	144

#	Article	IF	CITATIONS
181	Facile synthesis of ZrO2 coated BiOCl0.510.5 for photocatalytic oxidation-adsorption of As(III) under visible light irradiation. Chemosphere, 2018, 211, 934-942.	8.2	16
182	Degradation of petroleum hydrocarbons in seawater by simulated surface-level atmospheric ozone: Reaction kinetics and effect of oil dispersant. Marine Pollution Bulletin, 2018, 135, 427-440.	5.0	49
183	Dynamic kinetic asymmetric transformations of β-halo-α-keto esters by <i>N</i> , <i>N</i> ′-dioxide/Ni(<scp>ii</scp>)-catalyzed carbonyl-ene reaction. Chemical Communications, 2018, 54, 8901-8904.	4.1	15
184	Aligned N-doped carbon nanotube bundles with interconnected hierarchical structure as an efficient bi-functional oxygen electrocatalyst. RSC Advances, 2018, 8, 26004-26010.	3.6	11
185	Introducing Fe ²⁺ into Nickel–Iron Layered Double Hydroxide: Local Structure Modulated Water Oxidation Activity. Angewandte Chemie, 2018, 130, 9536-9540.	2.0	86
186	Introducing Fe ²⁺ into Nickel–Iron Layered Double Hydroxide: Local Structure Modulated Water Oxidation Activity. Angewandte Chemie - International Edition, 2018, 57, 9392-9396.	13.8	284
187	Phosphorus oxoanion-intercalated layered double hydroxides for high-performance oxygen evolution. Nano Research, 2017, 10, 1732-1739.	10.4	139
188	Synthetic Architecture of MgO/C Nanocomposite from Hierarchical-Structured Coordination Polymer toward Enhanced CO ₂ Capture. ACS Applied Materials & Interfaces, 2017, 9, 9592-9602.	8.0	57
189	Strong Metal–Phosphide Interactions in Core–Shell Geometry for Enhanced Electrocatalysis. Nano Letters, 2017, 17, 2057-2063.	9.1	145
190	A pomegranate-structured sulfur cathode material with triple confinement of lithium polysulfides for high-performance lithium–sulfur batteries. Journal of Materials Chemistry A, 2017, 5, 11788-11793.	10.3	23
191	Functional metal–organic framework boosting lithium metal anode performance via chemical interactions. Chemical Science, 2017, 8, 4285-4291.	7.4	164
192	Materials Chemistry of Iron Phosphosulfide Nanoparticles: Synthesis, Solid State Chemistry, Surface Structure, and Electrocatalysis for the Hydrogen Evolution Reaction. ACS Catalysis, 2017, 7, 4026-4032.	11.2	89
193	Mechanistic Insights into Surface Chemical Interactions between Lithium Polysulfides and Transition Metal Oxides. Journal of Physical Chemistry C, 2017, 121, 14222-14227.	3.1	86
194	Ultrathin dendrimer–graphene oxide composite film for stable cycling lithium–sulfur batteries. Proceedings of the National Academy of Sciences of the United States of America, 2017, 114, 3578-3583.	7.1	90
195	Selfâ€Cleaning Catalyst Electrodes for Stabilized CO ₂ Reduction to Hydrocarbons. Angewandte Chemie, 2017, 129, 13315-13319.	2.0	38
196	Selfâ€Cleaning Catalyst Electrodes for Stabilized CO ₂ Reduction to Hydrocarbons. Angewandte Chemie - International Edition, 2017, 56, 13135-13139.	13.8	126
197	A novel homozygous mutation in the FSHR gene is causative for primary ovarian insufficiency. Fertility and Sterility, 2017, 108, 1050-1055.e2.	1.0	32
198	High-performance Li–S battery cathode with catalyst-like carbon nanotube-MoP promoting polysulfide redox. Nano Research, 2017, 10, 3698-3705.	10.4	116

#	Article	IF	CITATIONS
199	Phase interactions in Mg-Ni-Al-O oxygen carriers for chemical looping applications. Chemical Engineering Journal, 2017, 326, 470-476.	12.7	31
200	A Meta-Analysis for Association of Maternal Smoking with Childhood Refractive Error and Amblyopia. Journal of Ophthalmology, 2016, 2016, 1-7.	1.3	8
201	Synthesis, Application, and Carbonation Behavior of Ca ₂ Fe ₂ O ₅ for Chemical Looping H ₂ Production. Energy & Fuels, 2016, 30, 6220-6232.	5.1	55
202	Ultrafine Alloy Nanoparticles Converted from 2D Intercalated Coordination Polymers for Catalytic Application. Advanced Functional Materials, 2016, 26, 5658-5668.	14.9	41
203	In situ studies of materials for high temperature CO ₂ capture and storage. Faraday Discussions, 2016, 192, 217-240.	3.2	12
204	High Performance Metal Oxide–Graphene Hybrid Nanomaterials Synthesized via Oppositeâ€Polarity Electrosprays. Advanced Materials, 2016, 28, 10298-10303.	21.0	24
205	A MnO ₂ /Graphene Oxide/Multi-Walled Carbon Nanotubes-Sulfur Composite with Dual-Efficient Polysulfide Adsorption for Improving Lithium-Sulfur Batteries. ACS Applied Materials & Interfaces, 2016, 8, 28566-28573.	8.0	77
206	Ferroceneâ€₽romoted Long ycle Lithium–Sulfur Batteries. Angewandte Chemie, 2016, 128, 15038-15042.	2.0	11
207	Ferroceneâ€Promoted Long ycle Lithium–Sulfur Batteries. Angewandte Chemie - International Edition, 2016, 55, 14818-14822.	13.8	46
208	Simultaneous removal of Cr(VI) and 4-chlorophenol through photocatalysis by a novel anatase/titanate nanosheet composite: Synergetic promotion effect and autosynchronous doping. Journal of Hazardous Materials, 2016, 317, 385-393.	12.4	92
209	Electrochemical CO ₂ Reduction to Hydrocarbons on a Heterogeneous Molecular Cu Catalyst in Aqueous Solution. Journal of the American Chemical Society, 2016, 138, 8076-8079.	13.7	450
210	Improving hydrogen yields, and hydrogen:steam ratio in the chemical looping production of hydrogen using Ca2Fe2O5. Chemical Engineering Journal, 2016, 296, 406-411.	12.7	61
211	Large scale computational screening and experimental discovery of novel materials for high temperature CO ₂ capture. Energy and Environmental Science, 2016, 9, 1346-1360.	30.8	61
212	Influence of surface capping on oxygen reduction catalysis: A case study of 1.7 nm Pt nanoparticles. Surface Science, 2016, 648, 120-125.	1.9	22
213	Structural evolution in synthetic, Ca-based sorbents for carbon capture. Chemical Engineering Science, 2016, 139, 15-26.	3.8	24
214	A highly active and stable hydrogen evolution catalyst based on pyrite-structured cobalt phosphosulfide. Nature Communications, 2016, 7, 10771.	12.8	418
215	One-Step Synthesis of MoS ₂ /WS ₂ Layered Heterostructures and Catalytic Activity of Defective Transition Metal Dichalcogenide Films. ACS Nano, 2016, 10, 2004-2009.	14.6	164
216	Development and performance of iron based oxygen carriers containing calcium ferrites for chemical looping combustion and production of hydrogen. International Journal of Hydrogen Energy, 2016, 41, 4073-4084.	7.1	60

#	Article	IF	CITATIONS
217	Lithiumâ€Ion Batteries: Countering Voltage Decay and Capacity Fading of Lithiumâ€Rich Cathode Material at 60 °C by Hybrid Surface Protection Layers (Adv. Energy Mater. 13/2015). Advanced Energy Materials, 2015, 5, .	19.5	2
218	Metal (Ni, Co)â€Metal Oxides/Graphene Nanocomposites as Multifunctional Electrocatalysts. Advanced Functional Materials, 2015, 25, 5799-5808.	14.9	490
219	Inhibiting the interaction between FeO and Al ₂ O ₃ during chemical looping production of hydrogen. RSC Advances, 2015, 5, 1759-1771.	3.6	72
220	Selective and irreversible adsorption of mercury(<scp>ii</scp>) from aqueous solution by a flower-like titanate nanomaterial. Journal of Materials Chemistry A, 2015, 3, 17676-17684.	10.3	71
221	Nickelâ€Rich Layered Lithium Transitionâ€Metal Oxide for Highâ€Energy Lithiumâ€Ion Batteries. Angewandte Chemie - International Edition, 2015, 54, 4440-4457.	13.8	1,512
222	Countering Voltage Decay and Capacity Fading of Lithiumâ€Rich Cathode Material at 60 °C by Hybrid Surface Protection Layers. Advanced Energy Materials, 2015, 5, 1500274.	19.5	172
223	Metal/Oxide Interface Nanostructures Generated by Surface Segregation for Electrocatalysis. Nano Letters, 2015, 15, 7704-7710.	9.1	233
224	Dual-Enhanced Photocatalytic Activity of Fe-Deposited Titanate Nanotubes Used for Simultaneous Removal of As(III) and As(V). ACS Applied Materials & Interfaces, 2015, 7, 19726-19735.	8.0	60
225	Ternary Hybrid Material for High-Performance Lithium–Sulfur Battery. Journal of the American Chemical Society, 2015, 137, 12946-12953.	13.7	253
226	Arsenate adsorption onto Fe-TNTs prepared by a novel water–ethanol hydrothermal method: Mechanism and synergistic effect. Journal of Colloid and Interface Science, 2015, 440, 253-262.	9.4	42
227	The performance of Fe2O3-CaO Oxygen Carriers and the Interaction of Iron Oxides with CaO during Chemical Looping Combustion and H2 production. Energy Procedia, 2014, 63, 87-97.	1.8	44
228	Nanostructured transition metal sulfides for lithium ion batteries: Progress and challenges. Nano Today, 2014, 9, 604-630.	11.9	545
229	Kinetics of the reduction of wüstite by hydrogen and carbon monoxide for the chemical looping production of hydrogen. Chemical Engineering Science, 2014, 120, 149-166.	3.8	63
230	Synergy of photocatalysis and adsorption for simultaneous removal of Cr(VI) and Cr(III) with TiO2 and titanate nanotubes. Water Research, 2014, 53, 12-25.	11.3	252
231	Flexural fatigue damage model of ultra-high toughness cementitious composites on base of continuum damage mechanics. International Journal of Damage Mechanics, 2014, 23, 949-963.	4.2	6
232	In a Nongenomic Action, Steroid Hormone 20-Hydroxyecdysone Induces Phosphorylation of Cyclin-Dependent Kinase 10 to Promote Gene Transcription. Endocrinology, 2014, 155, 1738-1750.	2.8	32
233	Adsorption mechanisms of thallium(I) and thallium(III) by titanate nanotubes: Ion-exchange and co-precipitation. Journal of Colloid and Interface Science, 2014, 423, 67-75.	9.4	94
234	Electrospun polyvinyl alcohol/waterborne polyurethane composite nanofibers involving cellulose nanofibers. Journal of Applied Polymer Science, 2014, 131, .	2.6	15

#	Article	IF	CITATIONS
235	Carbon nanotube-loaded mesoporous LiFe0.6Mn0.4PO4/C microspheres as high performance cathodes for lithium-ion batteries. Journal of Power Sources, 2014, 267, 459-468.	7.8	50
236	The hormone-dependent function of Hsp90 in the crosstalk between 20-hydroxyecdysone and juvenile hormone signaling pathways in insects is determined by differential phosphorylation and protein interactions. Biochimica Et Biophysica Acta - General Subjects, 2013, 1830, 5184-5192.	2.4	35
237	Fabrication of high tap density LiFe _{0.6} Mn _{0.4} PO ₄ /C microspheres by a double carbon coating–spray drying method for high rate lithium ion batteries. Journal of Materials Chemistry A, 2013, 1, 2411-2417.	10.3	76
238	A high performance oxygen storage material for chemical looping processes with CO ₂ capture. Energy and Environmental Science, 2013, 6, 288-298.	30.8	112
239	Reversible CO ₂ Absorption by the 6H Perovskite Ba ₄ Sb ₂ O ₉ . Chemistry of Materials, 2013, 25, 4881-4891.	6.7	17
240	Improvement of the high-temperature, high-voltage cycling performance of LiNi0.5Co0.2Mn0.3O2 cathode with TiO2 coating. Journal of Alloys and Compounds, 2012, 543, 181-188.	5.5	140
241	The Effect of Addition of ZrO ₂ to Fe ₂ O ₃ for Hydrogen Production by Chemical Looping. Industrial & Engineering Chemistry Research, 2012, 51, 16597-16609.	3.7	70
242	An investigation of the kinetics of CO2 uptake by a synthetic calcium based sorbent. Chemical Engineering Science, 2012, 69, 644-658.	3.8	81
243	A modified Al2O3 coating process to enhance the electrochemical performance of Li(Ni1/3Co1/3Mn1/3)O2 and its comparison with traditional Al2O3 coating process. Journal of Power Sources, 2010, 195, 8267-8274.	7.8	79